

- <sup>6</sup>L. V. Keldysh and Yu. V. Kopaev, *Fiz. Tverd. Tela (Leningrad)* **6**, 2791 (1964) [*Sov. Phys. Solid State* **6**, 2219 (1965)].  
<sup>7</sup>J. des Cloizeaux, *J. Phys. Chem. Solids* **26**, 259 (1965).  
<sup>8</sup>B. I. Halperin and T. M. Rice, *Solid State Phys.* **21**, 115 (1968).  
<sup>9</sup>E. A. Andryushyn and A. P. Silin, *Fiz. Nizk. Temp.* **3**, 1365 (1977) [*Sov. J. Low Temp. Phys.* **3**, 655 (1977)].  
<sup>10</sup>T. M. Rice, *Solid State Phys.* **32**, 1 (1977).  
<sup>11</sup>L. V. Keldysh and A. N. Kozlov, *Zh. Eksp. Teor. Fiz.* **54**,

- 978 (1968) [*Sov. Phys. JETP* **27**, 521 (1968)].  
<sup>12</sup>L. V. Keldysh and A. P. Silin, *Kratk. Soobshch. Fiz.* No. 8, 33 (1975).  
<sup>13</sup>A. P. Silin, *Fiz. Tverd. Tela (Leningrad)* **19**, 134 (1977) [*Sov. Phys. Solid State* **19**, 77 (1977)].  
<sup>14</sup>V. E. Bisti and A. P. Silin, *Fiz. Tverd. Tela (Leningrad)* **20**, 1850 (1978) [*Sov. Phys. Solid State* **20**, 1068 (1978)].

Translated by A. Tybulewicz

## The sign of the thermoelectric power in white tin

A. A. Altukhov, N. V. Zavaritskiĭ, and I. M. Suslov

*Institute of Physics Problems, USSR Academy of Sciences*  
 (Submitted 15 April 1980)  
*Zh. Eksp. Teor. Fiz.* **79**, 1518–1526 (October 1980)

The diffusion component of the thermoelectric power is investigated in the region of electron scattering by phonons. A value  $(\partial \ln S / \partial \ln \epsilon)_{\epsilon = \epsilon_F} = -1.5$  is obtained. It is shown that this value can be attributed to topological singularities of the Fermi surface of tin.

PACS numbers: 72.15.Jf, 72.10.Di, 71.25.Hc

The diffusion part of the thermoelectric power of a metal is defined by the expressions<sup>1</sup>

$$\alpha_s = \frac{\pi^2 k^2 T}{3e\epsilon_F} \xi = aT, \quad (1)$$

$$\xi = \left( \frac{\partial \ln \sigma}{\partial \ln \epsilon} \right)_{\epsilon = \epsilon_F} = \left( \frac{\partial \ln \Lambda}{\partial \ln \epsilon} + \frac{\partial \ln S}{\partial \ln \epsilon} \right)_{\epsilon = \epsilon_F}, \quad (2)$$

where  $\sigma$  is the conductivity of the metal,  $\Lambda$  is the electron mean free path, and  $S$  is the area of the Fermi surface (FS). We have shown in a preceding paper<sup>2</sup> that in the case of electron scattering by impurities the value of  $\xi$  is determined mainly by the first term of the right-hand side of (2) and depends on the type of impurity. For a pure metal (when electron-phonon scattering predominates), however, this question has so far remained unanswered. The point is that the experimental  $\xi$  for a number of polyvalent metals (gallium,<sup>3</sup> tin<sup>2</sup>) are essentially negative, and this is difficult to reconcile with the prevailing notions. In fact, as shown by Klemens,<sup>4</sup> in the isotropic case we have  $\partial \ln \tau / \partial \ln \epsilon = 0$ . The physical reason is that the energy relaxation is much faster than the momentum relaxation. It can therefore be assumed that  $\partial \ln \langle \tau \rangle / \partial \ln \epsilon$  will be small also in a weakly anisotropic case.

On the other hand, the FS of tin, as well as of most polyvalent metals, is in the broadened-band scheme close to a sphere of free electrons, for which  $\partial \ln \nu S / \partial \ln \epsilon = 3/2$ . The negative experimental  $\xi$  are therefore puzzling [ $\xi = -(1$  to  $3)$  for Sn].

Nielsen and Taylor<sup>5</sup> have shown recently that  $\partial \ln \tau / \partial \ln \epsilon$  can have large negative values on account of scattering processes in which virtual phonons participate. According to Ref. 2, however, the contribution they obtained for the pure metal cannot be significant at low temperatures.

In the present study we have attempted to resolve this contradiction in the case of tin, using the size effect for this purpose. The electron mean free path, which is governed by the finite dimensions of the sample, is independent of energy, and this makes it possible to estimate the contribution of both terms in the right-hand side of (2).

The theory of the size effect for electric conductivity was developed by Dingle.<sup>6</sup> It is known that in this theory a distinction is made between two limiting cases. For cylindrical samples at  $d \ll \Lambda_\infty$ , where  $d$  is the sample diameter and  $\Lambda$  is the electron mean free path in the bulk sample,

$$\rho_d / \rho_\infty = \Lambda_\infty / d. \quad (3)$$

Substituting  $\rho_d$  from (3) in (2), we readily obtain

$$a_d = \frac{\pi^2 k^2}{3e\epsilon_F} \frac{\partial \ln S}{\partial \ln \epsilon} = \text{const}(d). \quad (4)$$

For cylinders with  $d \gg \Lambda_\infty$

$$\rho_d / \rho_\infty = 1 + \gamma \Lambda_\infty / d. \quad (5)$$

From (5), (2), and (1) we have

$$a_d \rho_d = - \frac{\pi^2 k^2}{3e\epsilon_F} \left( \frac{\partial \rho_\infty}{\partial \ln \epsilon} - \frac{A}{d} \frac{\partial \ln S}{\partial \ln \epsilon} \right), \quad (6)$$

where

$$A = \gamma \rho_\infty \Lambda_\infty, \quad \frac{\partial \ln S}{\partial \ln \epsilon} = - \left( \frac{\partial \ln \rho_\infty}{\partial \ln \epsilon} + \frac{\partial \ln \Lambda_\infty}{\partial \ln \epsilon} \right).$$

It is seen from the presented relations that by measuring  $\rho$  and  $a$  as functions of the sample diameters we can determine  $\partial \ln \Lambda_\infty / \partial \ln \epsilon$  and  $\partial \ln S / \partial \ln \epsilon$ .

### EXPERIMENT

We investigated single crystals of ultrapure tin with  $\rho_{300 \text{ K}} / \rho_0 \geq 6 \cdot 10^5$ . The sample diameter ranged from 4 to

0.2 mm. The electron mean free path (determined from the residual resistivity of the bulk sample) was about 0.7 mm and three times larger than the diameter of the thinnest sample.

The technique of sample preparation and thermoelectric-power measurement was described before.<sup>2,7</sup> The thinnest samples were obtained by electrically etching a sample with initial diameter 0.6 mm. The sample used as the cathode was secured along the axis of the tin anode cylinder. The etching was in a continuous flow of electrolyte consisting of four parts of glacial acetic acid and one part of 30% hydrochloric acid (the density of the latter was 1.207 g/cm<sup>3</sup>). (The solution is explosive when dehydrated and heated!) The etching current was 1–2 A. The total etching time needed to decrease the diameter from 0.6 to 0.19 mm was ~50 hours. The measurements of  $\alpha_e$  were made without dismounting the sample from the etching setup.

### MEASUREMENT RESULTS

The measurements were made at temperatures 3.7–7.2 K. In this region, the phonon dragging is substantial, so that the total thermoelectric power is

$$\alpha = \alpha_e + \alpha_{ph} = aT + bT^2.$$

Just as in Ref. 2,  $\alpha_e$  was separated from  $\alpha_{ph}$  by using the dependence of  $\alpha/T$  on  $T^2$ . For dirty samples this dependence is linear with good accuracy,<sup>2</sup> but substantial deviations from linearity are possible in extremely pure samples. A typical plot of this dependence is shown in Fig. 1. At  $T > T^* \approx 5$  K the linearity is good, but at  $T < T^*$  the slope changes. The temperature  $T^*$  is, with good accuracy, that at which the phonon part and remaining parts of the electric resistance become equal. It is clear that electron scattering by residual impurities in the sample and by lattice defects come into play at  $T < T^*$ . To determine the thermoelectric power of the pure metal, however, it is necessary to investigate the part of the curve above  $T^*$ . The value obtained in this manner for a pure sample is  $\xi = -1.8$ . In our preceding paper<sup>2</sup> we did not take these factors into account using all the data in the reduction of the results. The value obtained for the same sample was then  $\xi = -3.6$  and was in fact listed in the "pure Sn" column of Table I there.

Simultaneously with the thermoelectric power we measured the resistivity of each sample. By plotting  $\rho_d$

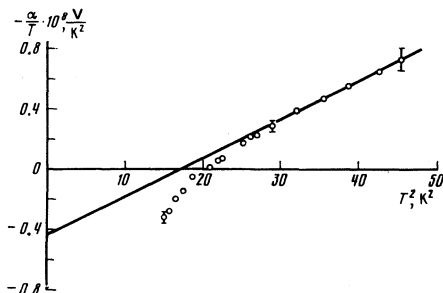


FIG. 1. Plot of  $\alpha/T$  against  $T^2$  for one of the pure tin samples ( $\rho_0 = 1.8 \times 10^{-10} \Omega\text{-cm}$ ). The straight line was drawn through the points at  $T > T^* = 5$  K.

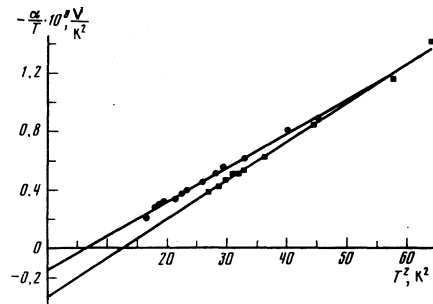


FIG. 2. Plot of  $\alpha/T$  against  $T$  for pure tin samples of different diameters:  $\bullet$   $d = 0.2$  mm,  $\blacksquare$   $d = 2$  mm.

against  $1/d$  we obtained  $\rho_\infty(0) = 1.6 \times 10^{-10} \Omega\text{-cm}$  and  $A = 1.3 \times 10^{-11} \Omega\text{-cm}^2$ , in agreement with the results of Aleksandrov *et al.*<sup>8,9</sup> It turned out that whereas the resistivities of the samples with  $d = 1$  mm and  $d = 0.19$  mm differ by almost seven times, the coefficients  $a_d$  differ only by a factor of two (Fig. 2). The experimental results are shown in Fig. 3a. Figure 3b shows a plot of  $a_d \rho_d$  against  $1/d$ , which agrees well (at  $d \geq \Lambda$ ) with relation (6). As a result we get

$$\partial \ln S / \partial \ln \epsilon = -1.5 \pm 0.3, \quad \partial \ln \Lambda_\infty / \partial \ln \epsilon = 0.4 \pm 0.3.$$

The value of  $\partial \ln \Lambda_\infty / \partial \ln \epsilon$  does not contradict Klemen's conclusion<sup>4</sup> that  $\partial \ln \tau / \partial \ln \epsilon = 0$ .

These estimates are based on the Dingle theory which presupposes, strictly speaking, an isotropic model. It may appear at first glance that the experimental result contradicts this premise, since a negative sign of  $\partial S / \partial \epsilon$  means that the FS is substantially nonspherical. Let us imagine, however, a FS in the form of a finely and uniformly grooved sphere. Such a surface is on the average isotropic (so long as  $d/\Lambda_\infty$  exceeds the characteristic angular dimension of the grooves), but can have arbitrary values of  $S$  and  $\partial S / \partial \epsilon$ . This means that the isotropy of the FS and the negative sign of  $\partial S / \partial \epsilon$  are in principle not contradictory. We note that the free-electron sphere of tin is strongly cut up by the Bragg planes (Fig. 4).

As  $d/\Lambda_\infty \rightarrow 0$  the indicated quasi-isotropy vanishes and Dingle's theory does not hold. This is manifest, in particular, by the fact that reduction by formula (4) yields a value of  $\partial \ln S / \partial \ln \epsilon$  that pertains not to the total sur-

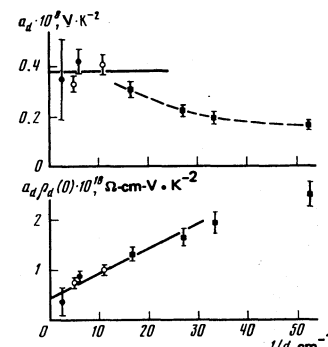


FIG. 3. a) Experimental dependence of  $a_d$  on  $1/d$  (the solid line characterizes the mean value in bulky samples), b) reduction of the experimental data in coordinates  $a_d \rho_d$  vs.  $1/d$ .

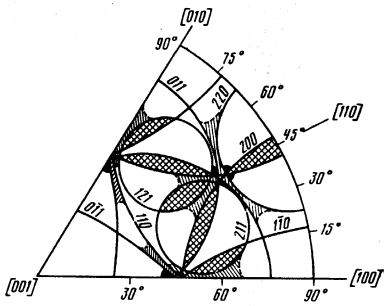


FIG. 4. Fermi surface of tin in the broadened-band scheme (conical equal-angle projection). The principal topological changes that distinguish it from the FS of free electrons are shown (according to the data of Ref. 10): filled-neck in fourth zone; cross-hatched vanishing of parts of the cigars in the fifth and sixth bands; dashed—striking to corner in third and fifth bands. The upper boundaries are drawn arbitrarily. The dashed sections of the sphere are missing from the real FS. Sections missing from the initial sphere but present on the real FS (they correspond to the electron “cube” of the sixth band) are not shown.

face, but to its local section in the direction of the sample axis. It is probable that this limit was not reached in the thickness interval investigated by us, as seen from Fig. 3a.

We examine now whether the obtained value  $\zeta = \partial \ln S / \partial \ln \epsilon$  can be reconciled with present-day notions concerning the FS of tin (Fig. 4). The possibility of  $\zeta$  having an arbitrary sign is usually connected with the presence of electron or hole surfaces. This explanation, however, calls for a major revision. It is known that according to Harrison's scheme the electron and hole surface are the results combining in one zone different sections of the free-electron sphere for which  $\zeta = +1$ . This process cannot change the value of  $\zeta$ ; the negative sign for the hole surfaces is offset by an increase of  $\zeta$  of the electron section, so that the net value of  $\zeta$  remains +1 as before. It is clear that the measurement of  $\zeta$  can be explained only by taking into account the deviations of the real Fermi surfaces from the free-electron model.

It is known that near the boundaries of the Brillouin zone the FS is rounded off in such a way that it crosses the zone boundaries at a right angle. The size of the roundoff is determined by the parameter  $\eta = |V_g|/\epsilon_F$ , where  $V_g$  is the Fourier component of the lattice pseudopotential; for most metals we have  $\eta \lesssim 0.1$  (for tin<sup>10</sup> we have  $\eta_{200} = 0.091$ ,  $\eta_{101} = 0.052$ ,  $\eta_{220} = 0.043$ ,  $\eta_{211} = 0.047$ ). The rounding-off leads to changes of  $S$  and  $\partial S/\partial \epsilon$ , which are proportional to  $\eta$  and are usually small. In fact, using the weak-coupling approximation formulas,<sup>11,12</sup> let us calculate the area of the rounded-off FS that crosses one Bragg plane. Then, assuming

$$\eta \ll 1, \quad \eta \ll \frac{k_F - g/2}{k_F} \quad (7)$$

we obtain

$$\frac{S}{S_0} = 1 - \frac{1}{2} \left( \frac{E(q)}{q} - \frac{1-q^2}{q} K(q) \right) \eta, \quad (8)$$

$$\frac{\partial S}{\partial \epsilon} / \frac{\partial S_0}{\partial \epsilon} = 1 + \frac{K(q) - E(q)}{4q} \eta, \quad q = \frac{g}{2k_F}.$$

where  $E(q)$  and  $K(q)$  are complete elliptic integral,  $g$  is the reciprocal-lattice vector, and  $S_0$  is the area of the Fermi surface. It is easy to verify that at any  $g/k_F$  the value of  $S$  decreases but  $\partial S/\partial \epsilon$  increases, i.e.,  $\zeta$  increases compared with +1. If the interference between the different Bragg planes is negligible, then the total change of  $S$  and  $\partial S/\partial \epsilon$  reduces to a sum over all the planes that cross the FS; it is clear that the value of  $\zeta$  for such a metal cannot be negative.<sup>1)</sup>

The interference between the planes is significant when the pseudopotential is large enough to permit a “topological change” of the FS compared with the free electrons. The “topological change” of the FS, according to Ref. 13, is defined as the change of its connectivity, viz., the vanishing or appearance of a pocket, or the breaking or formation of a neck. This definition implies the use of the reduced-zones scheme. In the broadened-bands scheme, the topological changes manifest themselves as the vanishing of individual sections of the sphere, as formation of contacts between the FS and the band boundaries, and others.

The topological-change process is called a phase transition of order  $2\frac{1}{2}$ .<sup>14</sup> This transition, as will be shown below, is accompanied by a jump of  $\partial S/\partial \epsilon$  in the case when a pocket vanishes, and by a jump with a logarithmic singularity of the  $\ln |\epsilon - \epsilon_c|$  type when a neck is broken ( $\epsilon_c$  is the energy at which the transition takes place).

The simplest topological change is shown in Fig. 5a. The Bragg planes cross the Fermi sphere at the very edge, and the sections cut off by the planes drop out by virtue of violation of the second condition of (7). It is easy to show that the associated change of  $\partial S/\partial \epsilon$  is given by

$$\delta \frac{\partial S}{\partial \epsilon} / \frac{\partial S_0}{\partial \epsilon} = -\frac{1}{2} + O(\eta), \quad (9)$$

i.e., it is of zero order in the pseudopotential. In fact, when two planes cross the sphere and the end pieces are made to vanish, we get a spherical segment whose logarithmic derivative is  $\frac{1}{2}$ , i.e.,  $\zeta$  is decreased by  $-\frac{1}{2}$ ; on the other hand the decrease of  $S$  and the roundoff produce a small effect  $\sim \eta$  [since  $(k_F - g/2)/k_F \sim \eta$ ]. If the

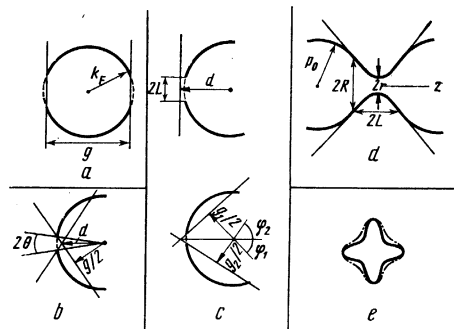


FIG. 5. Topological changes of Fermi surface (a—d) (dashed—vanished parts of the FS): a—vanishing of the segment cut off by the Bragg plane; b—vanishing of the section between two planes; c—sticking of FS to corner made up of two planes (2nd projection); d—onset of a neck; e—example of electron surface with negative  $\partial S/\partial \epsilon$  (dash-dot—surface at higher energy).

neck is not very thin, the manner in which it was broken does not matter—by vanishing of the cut-off sections ( $g < 2k_F$ ) or by “sticking” to the plane ( $g > 2k_F$ ).

We note that vanishing of arbitrarily small sections suffices to produce a finite change of  $\zeta$ . The reason is that at the instant of tangency a substantial change takes place in the energy dependence of the FS, and in place of  $S \propto \varepsilon$  for a sphere we get  $S \propto \varepsilon^{1/2}$  for a spherical segment. It is clear that when the sphere is intersected by several planes with  $g \approx 2k_F$  it is possible to have also  $\zeta < 0$ . This example shows that the negative sign of  $\zeta$  is not necessarily connected with the existence of hole surfaces. Moreover, one can visualize an essentially electronic surface (Fig. 5a) whose area decreases with increasing energy, whereas the volume increases. Such a surface has electron properties in the Hall and Nerst-Ettingshausen effects and hole properties in the thermoelectric power.<sup>2)</sup>

On the basis of the foregoing considerations, one should expect negative values of  $\zeta$  for noble metals (Cu, Ag, Au). This result was deduced from numerical calculations by Abarenkov and Vedernikov.<sup>15</sup> The possibility of decreasing  $\zeta$  of noble metals was discussed earlier by Ziman.<sup>16</sup>

In polyvalent metals, topological changes of the type shown in Fig. 5a are not typical and are rarely encountered (e.g., in Hg); the condition (7) is usually well satisfied for all Bragg planes with  $g < 2k_F$ . Even in this case, however, topological changes are possible of the line of intersection of two Bragg planes lies near the Fermi sphere, i.e.,

$$|k_F - d|/k_F \leq \eta,$$

where  $d$  is the shortest distance from the plane-intersection line to the center of the Fermi sphere. At  $k_F > d$  the topological change manifests itself in a vanishing of the section of the sphere between the planes (Fig. 5b), whereas at  $k_F < d$  it appears as a “sticking” of the FS to the corner (Fig. 5c). Calculating the area of the section of the sphere between the planes, we obtain for small  $\theta$  (Fig. 5b)

$$\frac{\delta S}{S_0} = -\frac{2^{\frac{1}{2}}}{3\pi} \left( \frac{1}{q^2} - 1 \right)^{\frac{1}{2}} \theta^{\frac{1}{2}},$$

$$\delta \frac{\partial S}{\partial \varepsilon} / \frac{\partial S_0}{\partial \varepsilon} = -\frac{1}{\sqrt{2}\pi} \left( \frac{1}{q^2} - 1 \right)^{-\frac{1}{2}} \theta^{\frac{1}{2}}.$$

Since the section can vanish at  $\theta \sim \eta$ , the corresponding changes of  $S$  and  $\partial S/\partial \varepsilon$  are of the order of  $\eta^{3/2}$  and  $\eta^{1/2}$ . Consequently, in this case, too, considerable changes of the logarithmic derivative of  $S$  can accompany very small changes of the area. In the FS of tin<sup>10</sup> there are no sections in the intersections of planes (200) and (020), (121) and (211), (200) and (101), or (110) and (211) (Fig. 4). The sections between (200) and (020) and their like made up the “cigar” of the fifth band in the FS of the free electrons; the remaining sections made up the cigars of the sixth band. At a total area of all the cigars  $\approx 0.1S_0$ , their vanishing makes a contribution of  $-3.0$  to the change of  $(\partial S/\partial \varepsilon)/(\partial S_0/\partial \varepsilon)$ .

To estimate the contribution of the sticking to the corner (Fig. 5c) we use the expression obtained for  $L$

from the three-wave approximation<sup>11</sup>

$$L = (p^2 - d^2 - 2m\lambda_0)^{\frac{1}{2}}, \quad (10)$$

where  $\lambda_0$  is the negative root of the equation

$$\lambda^3 - (V_1^2 + V_2^2 + V_3^2)\lambda - 2V_1V_2V_3 = 0,$$

$V_1$ ,  $V_2$ , and  $V_3$  are the Fourier components of the pseudopotentials corresponds to the wave vectors  $\mathbf{g}_1$ ,  $\mathbf{g}_2$ , and  $\mathbf{g}_1 - \mathbf{g}_2$ , respectively. Approximating the produced rounded regions by flat sections, we obtain

$$\delta \frac{\partial S}{\partial \varepsilon} / \frac{\partial S_0}{\partial \varepsilon} \approx \frac{1}{4\pi} \frac{\text{tg } \varphi_1 + \text{tg } \varphi_2}{\text{tg } \varphi_1 \text{tg } \varphi_2} \left\{ \frac{L}{p_F} - \frac{|\lambda_0| m}{p_F L} \right\}. \quad (11)$$

Since  $L \sim \eta^{1/2} p_F$  and  $\lambda \sim \eta \varepsilon_F$ , the contribution to  $\partial S/\partial \varepsilon$  is of the order of  $\eta^{1/2}$ , i.e., the same as in the preceding case; the contribution is usually positive. In Sn, sticking to a corner take place in the intersections of the planes (011) and (220), (110) and ( $\bar{1}01$ ), (121) and ( $\bar{1}21$ ), and (200) and (121). The first two correspond to breaks of the hole necks in the third band, and the remainder to vanishing of the gaps between the “pears” and the “double pancakes” in the fifth band.<sup>10</sup> An estimate by formula (11) shows that their total contribution does not exceed  $+2$ .

Topological changes can exist also in intersections of three and more planes (examples are the electron “cube” in the sixth band and the neck in the fourth band of Sn). It is difficult to estimate their contribution with the aid of the weak-coupling approximation, since this calls for allowance for a large number of plane waves. It is more convenient to go over in this case to the reduced-band scheme and use the general properties of the spectrum near the singular points.<sup>13</sup>

We consider now the formation of a small neck between two large parts of the FS (Fig. 5d). In view of the proximity to a conical singular point, the spectrum should take the form<sup>13</sup>

$$\varepsilon - \varepsilon_c = \frac{p_x^2}{2m_x} + \frac{p_y^2}{2m_y} - \frac{p_z^2}{2m_z} \quad (12)$$

(the  $z$  axis is along the neck axis, and the origin is at its center). The parameters  $m_x$ ,  $m_y$ ,  $m_z$  and  $\Delta = \varepsilon_F - \varepsilon_c$  can be estimated from the geometric dimensions of the neck, recognizing that at large  $p_z$  the neck should become joined to the large pear (Fig. 5d):

$$m_x = m_y \approx \frac{p_0}{p_F} m, \quad m_z \approx \frac{L^2}{R^2} m, \quad \Delta \approx \frac{r^2}{2m_x}$$

( $p_0$  is the radius of curvature of the large pear). The change of  $\partial S/\partial \varepsilon$  which occurs when the neck appears is

$$\delta \frac{\partial S}{\partial \varepsilon} / \frac{\partial S_0}{\partial \varepsilon} \approx -\frac{1}{2} \frac{p_0}{p_F} - \frac{1}{2} \frac{L}{p_F} \ln \frac{r}{p_0}. \quad (13)$$

For short necks ( $L \ll R$ ) only the first term is important, and agrees with (9) at  $p_0 = p_F$  (its exact value is  $m_x/2m$ ). For the two necks in the fourth zone of Sn we have  $L \ll R$  and  $p_0 \sim p_F$ , and their contribution to  $(\partial S/\partial \varepsilon)/(\partial S_0/\partial \varepsilon)$  is approximately  $-1$ .

In the case of long necks ( $L \gg R$ ) the second term of (13) is important. For example, sticking of a corner (Fig. 5c) in the reduced-band scheme looks like a break of a long hole neck ( $R \sim \eta p_F \ll L \sim \eta^{1/2} p_F$ ). In view of (13) its contribution to  $\partial S/\partial \varepsilon$  is  $\sim \eta^{1/2}$  and is positive in accord with the estimate above.

We can similarly estimate the onset (or vanishing) of a small electron pocket. The form of the spectrum near the minimum point is

$$e - \varepsilon_c \sim p^2/2m^*, \quad (14)$$

hence

$$\delta \frac{\partial S}{\partial \varepsilon} / \frac{\partial S_0}{\partial \varepsilon} \sim \frac{m^*}{m} \sim \frac{a^2}{2m\Delta}, \quad (15)$$

where  $a$  is the dimension of the pocket and  $\Delta = \varepsilon_F - \varepsilon_c$ . Usually a pocket produced near the intersection of a large number of planes has dimensions  $\sim \eta p_F$  in all directions; since  $\Delta \sim \eta \varepsilon_F$ , the corresponding contribution to  $\partial S/\partial \eta$  is  $\sim \eta$ . For example, for the electron cube in the sixth band, according to data of Ref. 10,  $a/p_F \approx 1/15$ , and  $\Delta/\varepsilon_F \approx 1/20$ , whence

$$\delta \frac{\partial S}{\partial \varepsilon} / \frac{\partial S_0}{\partial \varepsilon} \approx 1/10.$$

Gathering together all the contributions  $\sim 1$  and  $\eta^{1/2}$ , we obtain for Sn the value  $\partial \ln S / \partial \ln \varepsilon \approx -2$  [with allowance for the fact that according to an estimate by formula (8) we have  $S = 0.4S_0$ ]. Within the limits of the calculation accuracy this value agrees with that estimated from the experiment.

The anisotropy of  $\Lambda$  can influence the results in some way. In fact, let us take the most extreme case:  $\Lambda = 0$  for the electron sections, and is of the usual order of magnitude for the hole sections. Then all the kinetic coefficients are determined only by the hole surfaces, and  $\partial S/\partial \varepsilon$  turns out to be negative in the thermoelectric power and in the size effect. This artificial assumption, however, is in direct contradiction with the data on the size effect. Thus, resistance measurements yielded  $S = 0.43S_0$ , which agrees with the value obtained for the total area of the FS of tin by theoretical estimates [(0.4–0.5) $S_0$ , Ref. 12] and from other measurements [0.43 $S_0$  in Ref. 17, (0.50–0.55) $S_0$  in Ref. 12].

We note that in Refs. 15 and 16 it was assumed that the thermoelectric power is given by

$$\frac{\partial}{\partial \ln \varepsilon} \ln \int v dS,$$

and not by  $\partial \ln S / \partial \ln \varepsilon$ . The difference between these quantities corresponds to the assumption of constant  $\tau$  or of constant  $\Lambda$ . The presence of  $v$  under the integral sign does not affect the estimates significantly, since

the main contributions to  $\zeta$  are connected with the vanishing of the sections of the initial sphere.

Thus, with tin as an example, it has been shown that in polyvalent metals small topological changes of the real Fermi surface, compared with the Fermi surface of the almost-free-electron model, can lead to substantial changes of  $\partial \ln S / \partial \ln \varepsilon$ .

<sup>1</sup>Exceptions are possible in the case of a strong energy dependence of the pseudopotential. For Sn, however, the corresponding corrections are small and also lead to an increase of  $\zeta$  (a calculation of the energy dependence of the pseudopotentials is described in Ref. 2).

<sup>2</sup>The authors thank M. I. Kaganov for pointing out this circumstance.

<sup>1</sup>J. M. Ziman, *Electrons and Phonons*, Oxford, 1960.

<sup>2</sup>A. A. Altukhov, Yu. K. Dzhikaav, N. V. Zavaritskiĭ, and I. M. Suslov, *Zh. Eksp. Teor. Fiz.* **75**, 2256 (1978) [*Sov. Phys. JETP* **48**, 1137 (1978)].

<sup>3</sup>S. N. Mahajan, I. G. Daunt, R. I. Boughton, and M. Yagub, *Low Temp. Phys.* **12**, 347 (1973).

<sup>4</sup>P. G. Klemens, *Physica* **69**, 171 (1973).

<sup>5</sup>P. E. Nielsen and P. L. Taylor, *Phys. Rev.* **B10**, 4061 (1974).

<sup>6</sup>R. B. Dingle, *Proc. Roy. Soc.* **A201**, 545 (1950).

<sup>7</sup>N. V. Zavaritskiĭ and A. A. Altukhov, *Zh. Eksp. Teor. Fiz.* **70**, 1861 (1976) [*Sov. Phys. JETP* **43**, 969 (1976)].

<sup>8</sup>B. N. Aleksandrov and B. I. Verkin, *ibid.* **34**, 1655 (1958) [7, 1137 (1958)].

<sup>10</sup>M. D. Stafleu and A. R. de Vroomen, *Phys. St. Sol.* **23**, 683 (1967).

<sup>11</sup>W. A. Harrison, *Pseudopotentials in the Theory of Metals*, Benjamin, 1966.

<sup>12</sup>G. P. Motulevich, *Opticheskie svoĭstva metallov. Mezhmolekulyarnoe vzaimodeĭstvie* (Optical Properties of Metals. Intermolecular Interaction). *Trudy FIAN, Nauka*, 1971.

<sup>13</sup>I. M. Lifshitz, M. Ya. Azbel', and M. I. Kaganov, *Elektronnaya teoriya metallov* (Electron Theory of Metals), Nauka, 1971, § 2 [Consultants Bureau, 1973].

<sup>14</sup>M. I. Kaganov and I. M. Lifshitz, *Usp. Fiz. Nauk* **129**, 487 (1979) [*Sov. Phys. Usp.* **22**, 904 (1979)].

<sup>15</sup>A. V. Abarenkov and M. V. Vedernikov, *Fiz. Tverd. Tela* (Leningrad) **8**, 236 (1966) [*Sov. Phys. Solid State* **8**, 186 (1966)].

<sup>16</sup>J. M. Ziman, *Adv. Phys.* **10**, 1 (1961).

<sup>17</sup>R. G. Chambers, *Proc. Roy. Soc.* **A215**, 481 (1952).

Translated by J. G. Adashko